Food and Chemical Toxicology 129 (2019) 391–398

Contents lists available at ScienceDirect

Food and Chemical Toxicology

journal homepage: www.elsevier.com/locate/foodchemtox

Development of a two-layer transwell co-culture model for the *in vitro* investigation of pyrrolizidine alkaloid-induced hepatic sinusoidal damage

Yao Lu[1], Jiang Ma[1], Ge Lin[*]

School of Biomedical Sciences, Faculty of Medicine, The Chinese University of Hong Kong, Hong Kong, China

ARTICLE INFO

Keywords:
Pyrrolizidine alkaloid
Hepatic sinusoidal damage
Transwell co-culture model
In vitro cell model
HepaRG hepatocytes

ABSTRACT

Pyrrolizidine alkaloids (PAs) are hepatotoxic and specifically damage hepatic sinusoidal endothelial cells (HSECs) via cytochrome P450 enzymes (CYPs)-mediated metabolic activation. Due to the lack of CYPs in HSECs, currently there is no suitable cell model for investigating PA-induced HSEC injury. This study aimed to establish a two-layer transwell co-culture model that mimics hepatic environment by including HepaRG hepatocytes and HSECs to evaluate cytotoxicity of PAs on their major target HSECs. In this model, PAs were metabolically activated by CYPs in HepaRG hepatocytes to generate reactive pyrrolic metabolites, which react with co-cultured HSECs leading to HSEC damage. Three representative PAs, namely retrorsine, monocrotaline, and clivorine, induced significant concentration-dependent cytotoxicity in HSECs in the co-culture model, but did no cause obvious cytotoxicity directly in HSECs. Using the developed co-cultured model, further mechanism studies of retrorsine-induced HSEC damage demonstrated that the reactive pyrrolic metabolite generated by CYP-mediated bioactivation in HepaRG hepatocytes caused formation of pyrrole-protein adducts, reduction of GSH content, and generation of reactive oxygen species in HSECs, leading to cell apoptosis. The established co-culture model is reliable and applicable for cytotoxic assessment of PA-induced HSEC damage and offers a novel platform for screening toxicity of different PAs on their target cells.

1. Introduction

Pyrrolizidine alkaloids (PAs) are among the most significant groups of phytotoxins and widely present in about 3% of flowering plants, especially those from the plant families of Asteraceae, Boraginaceae and Fabaceae (Fu et al., 2004; Roeder, 1995, 2000). More than 660 PAs have been found in over 6000 plants including those used as herbal medicines for the treatment of traumatic injury, pain, inflammation and other ailments (Edgar et al., 2015; Roeder, 2000). Approximately half of these PAs have been reported to be hepatotoxic in livestock and human. PA poisoning cases have been constantly reported due to the intake of PA-producing herbal products or PA-contaminated foodstuffs (Gao et al., 2015; Lin et al., 2011; Mohabbat et al., 1976; Prakash et al., 1999; Robinson et al., 2014; Ruan et al., 2015; Willmot and Robertson, 1920).

PAs are esters of three types of necine bases including retronecine-type, otonecine-type, and platynecine-type. Retronecine-type and otonecine-type PAs containing unsaturated necine bases are toxic, while platynecine-type PAs possessing a saturated necine base are considered to be non/less-toxic (Edgar et al., 2015; Fu et al., 2004; Li et al., 2011; Lin et al., 2000; Ruan et al., 2014a, 2014b). Metabolic activation catalyzed by hepatic cytochrome P450 enzymes (CYPs), especially CYP3A family, is a prerequisite for PAs to exert their toxicities. Toxic PAs are metabolized into their reactive pyrrolic metabolites known as dehydro-PAs, which are highly reactive and can rapidly bind covalently with cellular proteins to form pyrrole-protein adducts and impair the function of critical proteins leading to hepatotoxicity, particularly in hepatic sinusoidal endothelial cells (HSECs) known as hepatic sinusoidal obstruction syndrome (HSOS) (Fig. 1) (Fu, 2017; Fu et al., 2001, 2004; Kim et al., 1995; Li et al., 2011; Lu et al., 2018; Ma et al., 2018; Mattocks, 1968; Xia et al., 2013; Yang et al., 2016; Zhao et al., 2012; Zhu et al., 2017). Dehydro-PAs also react with glutathione (GSH) to form readily excreted pyrrole-GSH conjugates (Fig. 1). Thus, glutathione conjugation is generally considered as a detoxification pathway (Fu et al., 2004; Li et al., 2011; Yan and Huxtable, 1995). On the other hand, excessive reaction with GSH may severely deplete cellular GSH. It has been reported that the reduced cellular GSH content along with the increased oxidative stress is one of the important causes of PA-induced cytotoxicity (DeLeve et al., 1996; Ji et al., 2009; Wang et al., 2000).

[*] Corresponding author.
E-mail address: linge@cuhk.edu.hk (G. Lin).
[1] Author Contributions: These authors contributed equally to this work.

https://doi.org/10.1016/j.fct.2019.04.057
Received 1 March 2019; Received in revised form 26 April 2019; Accepted 29 April 2019
Available online 02 May 2019

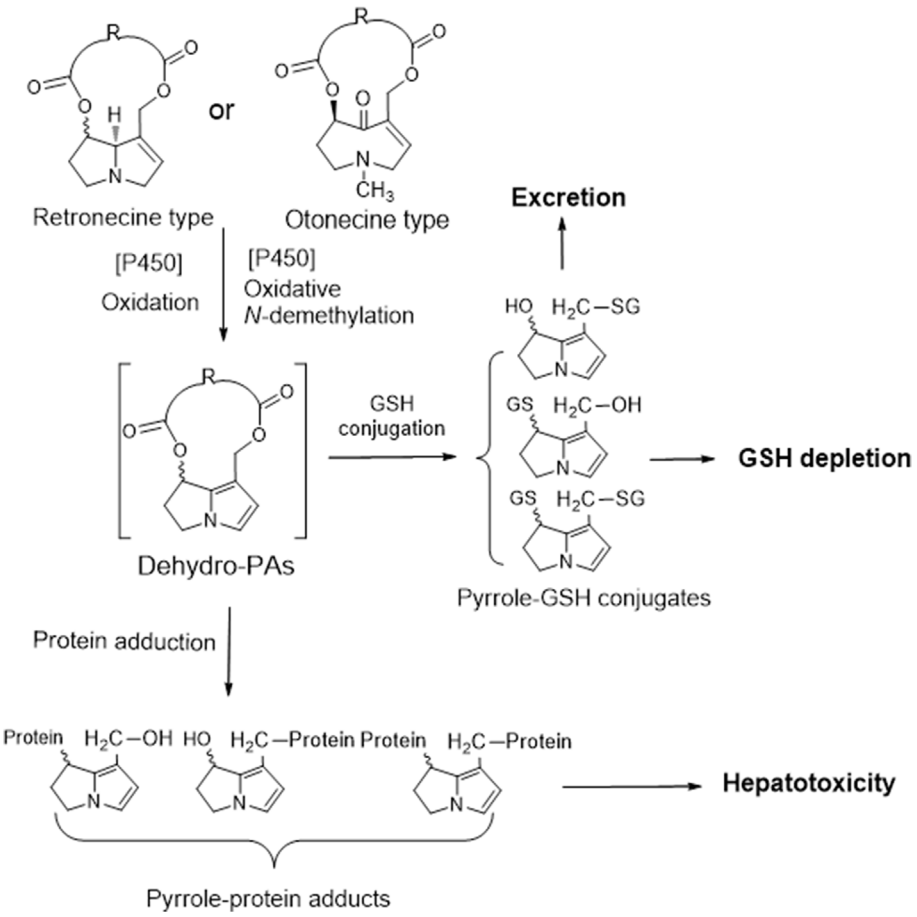

Fig. 1. Metabolic activation of retronecine-type and otonecine-type toxic PAs resulting in formation of dehydro-PAs which further interact with cellular glutathione (GSH) or proteins to generate pyrrole-GSH conjugates or pyrrole-protein adducts leading to hepatotoxicity. The excessive amount of dehydro-PAs formed may deplete cellular GSH, enhancing hepatotoxicity.

HSOS presents as an initial obstruction in the hepatic sinusoids followed by dilation of sinusoids and sinusoidal hemorrhage (DeLeve et al., 1999, 2003a; DeLeve et al., 2003b). HSECs are considered as the major target cells involving in the PA-induced HSOS (DeLeve et al., 1996, 2002, 2003a). HSEC itself, however, lacks CYPs essential for the bioactivation of PAs. Major CYP isoforms that are responsible for metabolic activation of PAs, such as CYP3A4, CYP3A5 and CYP2A6, are extremely low or not expressed in HSECs. Therefore, PAs cannot directly exert cytotoxicity in HSECs. It is well-studied that hepatocytes, which express high level of CYPs, bioactivate PAs to form dehydro-PAs, which subsequently exposes to adjacent HSECs in the liver leading to HSEC damage. Heretofore, due to the fact that HSECs with CYP deficiency are unable to metabolically activate PAs, the suitable *in vitro* model for the study of PA-induced HSEC damage is still lacking, which has obscured the investigation of different PAs induced damage in HSECs and its underlying mechanism. Therefore, the aim of the present study was to develop a two-layer transwell co-culture model that included both hepatocytes and HSECs for the investigation of PA-induced HSEC damage. In this model, human HepaRG hepatocytes and HSECs were cultured on bottom surface and top surface of a microporous membrane, respectively. HepaRG hepatocytes closely resemble normal properties of human primary hepatocytes, especially its ability of metabolizing CYPs substrates, including PAs. Several studies have demonstrated that HepaRG hepatocytes have comparable metabolizing activities of various CYPs, especially CYP3A4 isozyme, to that found in human hepatocytes, suggesting their use in drug metabolism (Lübberstedt et al., 2011; McGill et al., 2011). In the developed two-layer transwell co-culture model, PAs could be metabolically activated by CYPs present in HepaRG hepatocytes to generate dehydro-PAs, which diffused into the top-surface and then form pyrrole protein-adducts leading to cytotoxicity in HSECs. This model offers a functional resemblance mimicking *in vivo* hepatic environment and allows us to study the toxic effects of different PAs on HSECs in a more realistic manner.

2. Materials and methods

2.1. Chemicals and materials

Retrorsine and monocrotaline were purchased from the Sigma-Aldrich (St. Louis, USA). Clivorine was isolated in our laboratory from *Ligularia hodgsonii*. Transwell® plates (pore size of microporous membrane: 0.4 μm) were purchased from Costar® (Corning®, USA). Williams' Medium E, Hank's Balanced Salt Solution, glutamine (GlutaMAX™), fetal bovine serum (FBS), and CellROX® Green Reagent (for oxidative stress detection) were purchased from Thermo Fisher Scientific Inc (MA, USA). Endothelial cell medium (ECM) and endothelial cell growth supplement were obtained from ScienCell Research Laboratories (CA, USA). HPLC-grade ethanol, acetone, formic acid, and acetonitrile were purchased from Merck (Darmstadt, Germany). Cell Counting Kit-8 (CCK-8) was obtained from Dojindo Laboratories (Kumamoto, Japan). The Caspase-Glo® 3/7 activity assay kit was purchased from Promega (Promega, USA). Annexin V-fluorescein isothiocyante (FITC) Apoptosis Detection Kit was obtained from Biotool (Houston, USA). Other chemicals, including hydrocortisone hemisuccinate, dimethyl sulfoxide (DMSO), human insulin, sulfosalicylic acid, 5,5′-dithiobis-2-nitrobenoic acid (DTNB), glutathione disulfide (GSSG) reductase, nicotinamide adenine dinucleotide phosphate (NADPH), silver nitrate, 4-(dimethylamino)benzaldehyde, and perchloric acid were all purchased from Sigma-Aldrich (St. Louis, USA).

2.2. Cell culture and treatment

Human HSECs were purchased from ScienCell Research Laboratories (CA, USA). HSECs were cultured in ECM supplemented with 5% FBS and 1% endothelial cell growth supplement according to the manufacture's protocol. Human HepaRG hepatocytes were obtained from Biopredic International (Rennes, France) and were authorized for use in the study through a material transfer agreement. HepaRG hepatocytes were cultured in HepaRG growth medium composed of Williams' Medium E mixed with 10% FBS, 100 units/ml penicillin, 100 μg/ml streptomycin (Thermal Fisher), 5 μg/ml insulin, 2 mM glutamine, 1 × MEM Non-Essential Amino Acids Solution (Thermal Fisher) and 50 μM hydrocortisone hemisuccinates. The cells were passaged every 14 days at a density of 2.5×10^4 cells/cm^2 in a T75 flask (Corning®, USA). Two weeks after seeding, DMSO (final concentration 1.5%) was added to the HepaRG growth medium to induce hepatocyte differentiation for 2 weeks. Differentiated hepatocytes with a high activity of CYPs were detached by trypsinization and re-suspended in the culture medium and seeded with a high density of 2×10^5 cells/cm^2 in multi-well culture plates in a humidified CO_2 incubator (37 °C, 95% air and 5% CO_2) prior to the use of two-layer transwell co-culture model.

2.3. Set-up of two-layer transwell co-culture model

The two-layer transwell co-culture model was established based on the modification of a previously published method by co-culturing primary rat hepatocytes and primary rat liver sinusoidal endothelial cells (Kang et al., 2013). In the present model, HepaRG hepatocytes and HSECs were co-cultured on bottom and top surface of transwell microporous membrane, respectively. The detailed procedures for constructing the two-layer transwell co-culture model are illustrated in Fig. 2a. Firstly, a transwell insert with microporous membrane was carefully wrapped around the edge of its microporous membrane using the sterilized parafilm (Parafilm M®, USA) to build a parafilm fence, which could hold up to 1 mL medium. Differentiated HepaRG hepatocytes (2×10^5 cells/cm^2) were then plated on bottom side of transwell insert membrane for a minimum incubation of 6 h in HepaRG culture medium at 37 °C in 5% CO_2 to allow the cells to firmly attach to the microporous membrane. After HepaRG hepatocytes being firmly attached to the microporous membrane, the transwell insert was then turned over and put back to the well plate to allow HepaRG hepatocyte-plated side of the membrane to face down. Finally, HSECs (4×10^4 cells/cm^2) were seeded onto top side of transwell insert membrane. The resultant transwell plate was then incubated in ECM for a minimum of 12 h at 37 °C in 5% CO_2. Thus, HepaRG hepatocytes formed the first layer on bottom side of the membrane and human HSEC cells formed the second layer on the top side of the membrane, and the two layers were isolated by the microporous membrane, but the medium could diffuse freely across the membrane.

2.4. CYP3A4 activity of HepaRG hepatocytes cultured in ECM

The major purpose for creating this *in vitro* model was to investigate cytotoxic effect of PAs in HSECs. In the established two-layer transwell co-culture model, in order to maintain optimal morphology and viability of HSECs, two types of cells had to be cultured in HSECs favorable medium ECM. However, whether HepaRG hepatocytes could maintain CYP3A4 activity in ECM is unknown and needed to be confirmed, because a high and reproducible activity of CYPs, especially activity of CYP3A4, is essential for metabolic activation of PAs and thus plays a critical role in PA-induced HSOS damage. The activity of CYP3A4 in HepaRG hepatocytes was evaluated by measuring oxidative metabolism of nifedipine (a specific CYP3A4 substrate) to produce oxidized nifedipine (the metabolite specifically produced by CYP3A4-mediated oxidation of nifedipine). In two-layer transwell co-culture model, HepaRG hepatocytes and HSECs or both will be individually cultured or co-cultured for different times (0–48 h) prior to the incubation with nifedipine for 1 h. Afterwards, an aliquot (200 μL) of ECM was collected from the insert and mixed with the same volume of ice-cold methanol to precipitate the proteins, followed by measurement ofoxidized nifedipine by LC-MS. Briefly, an Agilent 6460 Triple Quadrupole LC/MS System coupled with an Agilent ZORBAX Eclipse Plus C_{18} column (2.1 × 100 mm, 1.8 mm) was applied. A mixture of acetonitrile: 0.1% formic acid water (85:15, v/v) was used as mobile phase at a flow rate of 0.3 mL/min. The mass spectrometer was operated in positive mode. The multiple reaction monitoring (MRM) model was chosen for quantification of nifedipine and oxidized nifedipine (MRM transition: nifedipine *m/z* 347.1-315.0 and oxidized nifedipine *m/z* 345-284.2).

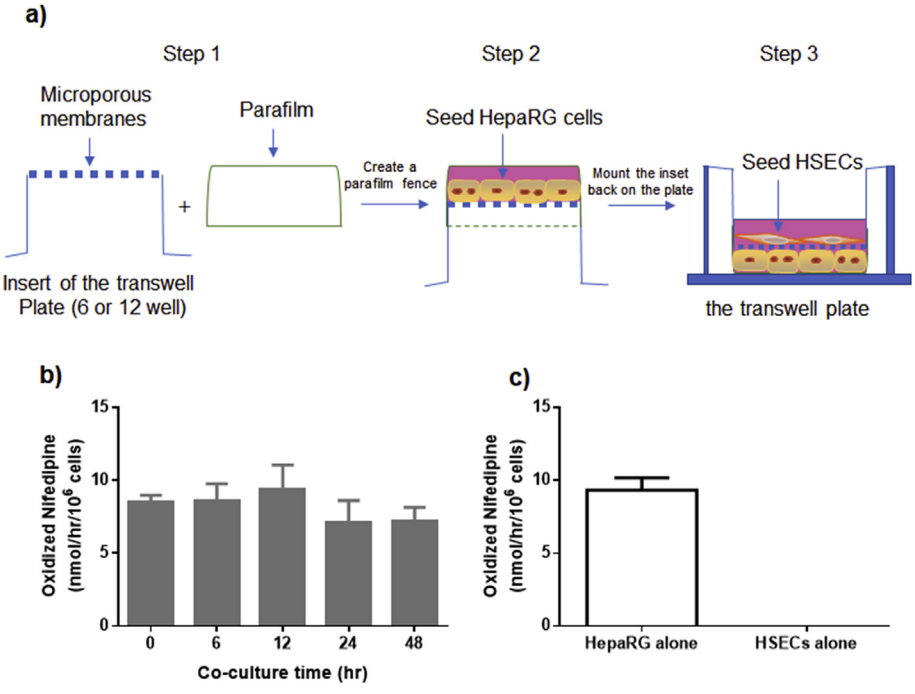

Fig. 2. Sketched procedures to prepare a two-layer transwell co-culture model. HepaRG hepatocytes and HSECs were co-cultured on bottom and top surface of transwell microporous membrane, respectively. These two types of cells were separated by the microporous membrane that mimicked the space of Disse (a). Formation of oxidized nifedipine (the metabolite specifically produced by CYP3A4-mediated oxidation of nifedipine (a specific CYP3A4 substrate)) for 1 h incubation of nifedipine in HeapRG hepatocytes and HSECs (b), and HeapRG hepatocytes or HSECs alone (c) in the co-culture model. Prior to the 1 h incubation of nifedipine, HepaRG hepatocytes and HSECs were co-cultured in the developed model for different times (0–48 h) to investigate the maintenance of metabolic activity of HepaRG hepatocytes cultured in ECM (b), or individually cultured for 12 h to compare the metabolic activity of HepaRG hepatocytes and HSECs (c). Data are expressed as mean ± SD (n = 3).

2.5. Cell viability assay

HSECs were treated with different concentrations of retrorsine, monocrotaline or clivorine dissolved in ECM containing DMSO (0.5% final concentration) or ECM containing 0.5% DMSO as solvent controls in two-layer transwell co-culture model for 24 h. After treatment, parafilm fence was removed from the edge of the insert. HepaRG hepatocytes were carefully wiped off by a cotton robe, and HSECs remained on top side of the microporous membrane. Cell viability of HSECs was detected using Cell Counting Kit-8 (CCK-8) by following manufacture's protocol. Briefly, CCK-8 reagent solution was diluted 5 times by ECM to form the reagent mixture, which replaced the incubated ECM in each insert in the transwell plate. The transwell plate was then incubated at 37 °C for 45 min, and optical density (OD) value in each insert was read at wavelength 450 nm on a microplate reader (Molecular Devices, Sunnyvale, USA). The cell viability was calculated based on the following formula:

$$\text{Cell viability}\ (\%) = \frac{\text{OD}(treatment) - \text{OD}(blank)}{\text{OD}(control) - \text{OD}(blank)} \times 100$$

2.6. Determination of GSH level in HSECs

The GSH content in retrorsine-treated HSECs was determined using modified DTNB-GSSG reductase recycling assay (Dehn et al., 2004). In brief, after retrorsine treatment for 24 h in two-layer transwell co-culture model, HSECs were trypsinized and collected from the transwell by centrifugation at 500*g* and then lysed in 10 mM hydrogen chloride with 1% sulfosalicylic acid. Subsequently, 20 μL supernatant was mixed with 250 μL of reaction mixture containing 0.7 mM DTNB, 1.2 U/L GSSG reductase, and 0.24 mM NADPH. The enzymatic reaction kinetic was evaluated for 0–2.5 min at 415 nm on a microplate reader. The rate of the reaction was measured and GSH concentration was determined from the standard curve. Protein concentrations of the samples were determined using bicinchoninic acid assay (Smith et al., 1985).

2.7. Detection of reactive oxidative stress in HSECs

CellROX® Green Reagen was diluted from its original stock concentration of 2.5 mM by 1000 folds using ECM (in the presence or absence of 120 μM retrorsine) to achieve the final concentration of 2.5 μM. Retrorsine (120 μM) was treated in two-layer transwell co-culture model for 3 h. After removing HepaRG hepatocytes, HSECs were incubated with CellROX® Green Reagen for 1 h at 37 °C. At the end of the incubation, medium was removed, and cells were washed twice with Hank's Balanced Salt Solution and collected by trypsinization and centrifugation at 400*g* for 3 min. The collected cells were resuspended in 0.5 μL of cold ECM and kept on ice for the further flow cytometry analysis. Fluorescence excitation and emission wavelength were set at 488 nm and 530 nm, respectively, for the flow cytometry analysis.

2.8. Determination of pyrrole–protein adducts in HSECs

The content of pyrrole-protein adducts in HSECs was quantified according to our previously published method (Ruan et al., 2014b, 2015). In brief, after the treatment of different concentrations of retrorsine for 24 h in two-layer transwell co-culture model, HSECs were trypsinized and collected from the transwell. To the obtained cell pellets, 100 μL of ice-cold acetone was added, vortexed, ultrasonicated for 10–20 s, and centrifuged at 3,000 *g* for 10 min to produce the total protein pellets. After washing with absolute ethanol, the protein pellets were reconstituted into 5 vol of 2% acidic silver nitrate ethanol solution and shaken for 30 min, followed by centrifugation at 20,000 *g* for 5 min. The resultant supernatant was reacted with 4-(dimethylamino)benzaldehyde (v/v 4:1) in ethanol at 55 °C for 10 min. The mixture obtained was subjected to LC–MS analysis using our previously developed method (Ruan et al., 2014b, 2015).

2.9. Quantification of apoptosis of HSECs

The apoptosis assay was conducted by using Annexin V-FITC Apoptosis Detection kit (Houston, USA). Briefly, after retrorsine (120 μM) treatment in two-layer transwell co-culture model for 24 h, HSECs harvested by trypsinization and centrifugation at 200*g*. Cell pellets were then washed with cold phosphate-buffered saline, centrifuged, and resuspended in 100 μL binding buffer provided by the detection kit. A mixture of 5 μL Annexin V-FITC and 5 μL propidium iodide staining solution was added to each 100 μL of cell suspension to incubate at room temperature for 15 min for staining. After the incubation, 400 μL of ice-cold binding buffer was added to the cell suspension, and then analyzed by LSR II flow cytometry (BD Biosciences) with fluorescence emission at 530 nm and 590 nm.

2.10. Caspase-3/7 activity assay

The cellular caspase-3/7 activity was quantified using Caspase-Glo® 3/7 assay kit (Promega, Singapore) per vender's protocol. After retrorsine (120 μM) treatment in two-layer transwell co-culture model for 24 h, HSECs were collected and lysed with the assay reagent provided by the kit, followed by incubation at room temperature for 1 h. The luminescence intensity of the cell lysis was recorded by SpectraMax® i3 Multimode 6–384 Plate Reader. Luminescence emitted from cell lysis was proportional to the amount of caspase activity present. The activity of caspase-3/7 was expressed as a ratio of luminescence intensity of the retrorsine-treated samples to that of the corresponding controls.

2.11. Data and statistical analysis

All data are expressed as mean ± SD. One-way ANOVA with Bonferroni post hoc test and Student's t-test were used for the comparison among various groups and between two groups respectively. Statistical significance was set at $p < 0.05$. All statistics were performed using either PASW Statistics (version 18) or GraphPad Prism 6.

3. Results

3.1. Develops a two-layer transwell co-culture model

The procedures of establishing a two-layer transwell co-culture model which includes both HepaRG hepatocytes and HSECs for evaluating cytotoxicity of PAs on HSECs were illustrated in Fig. 2a. Given the importance of metabolic capability of HepaRG hepatocytes in this model and the important role played by CYP3A4 in metabolic activation of PAs, CYP3A4 enzyme activity of HepaRG hepatocytes was measured by using its classic substrate, nifedipine, to evaluate how long HepaRG hepatocytes were able to maintain its metabolic activity during co-culture with HSECs in ECM. The results shown in Fig. 2b demonstrated that after co-culture of both types of cells in ECM for 0–48 h in two-layer transwell co-culture model, the 1 h formation of CYP3A4-mediated nifedipine metabolite, oxidized nifedipine, were unchanged, indicating that CYP3A4 activity of HepaRG hepatocytes maintained for at least 48 h in the developed two-layer transwell co-culture model. On the other hand, for 1 h CYP3A4-mediated metabolism in individual cell types, HepaRG hepatocytes produced similar amount of oxidized nifedipine to that generated in two-layer transwell co-culture model, while HSECs did not metabolize nifedipine to oxidized nifedipine (Fig. 2c), confirming the lack of CYP3A4 activity in HSECs. The results demonstrated that a two-layer transwell co-culture mode having HSECs and HepaRG hepatocytes with maintained CYP3A4 activity was developed and ready for the *in vitro* study of cytotoxic effects of PAs on HSECs.

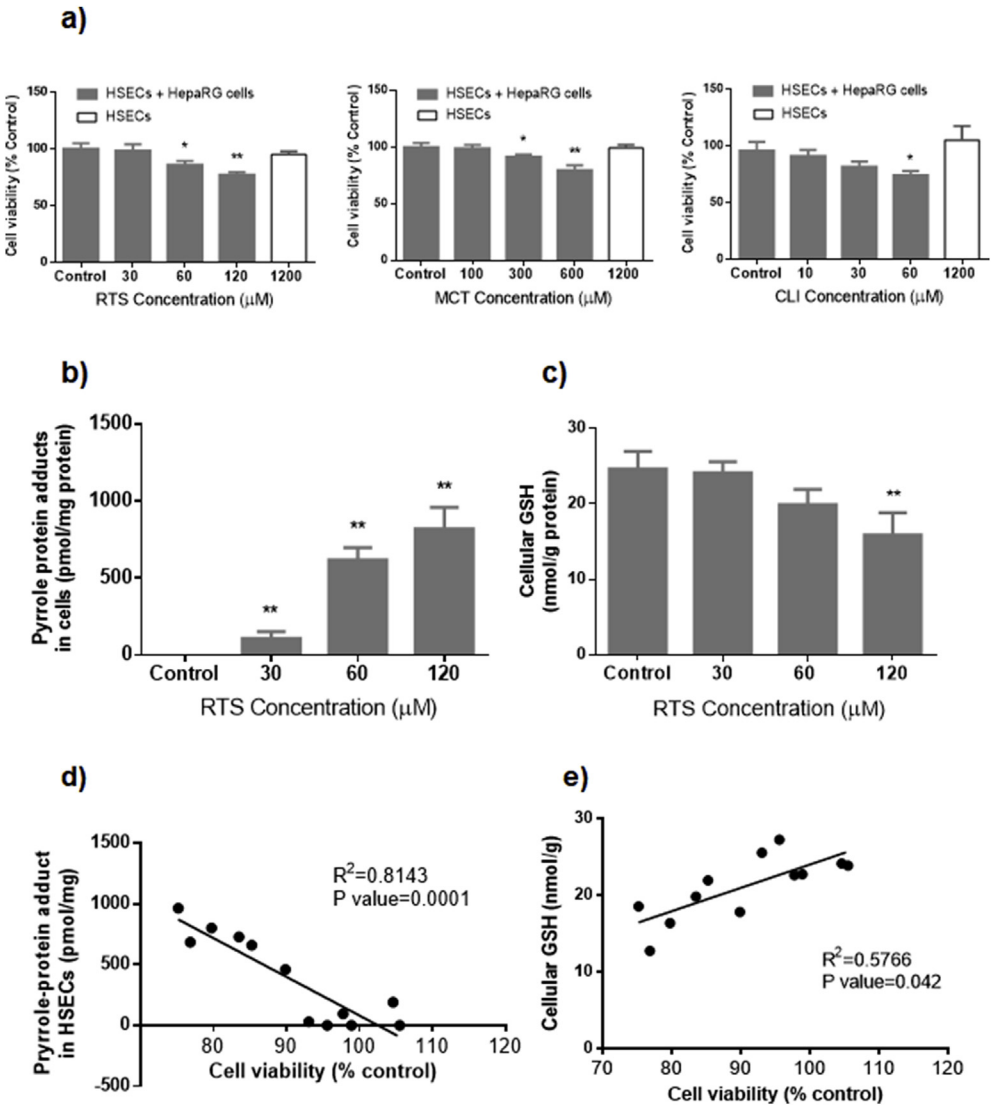

Fig. 3. Effects of 24 h treatment of retrorsine (RTS), monocrotaline (MCT) and clivorine (CLI) on the viability of HSECs in the presence or absence of HepaRG hepatocytes in two-layer transwell co-culture model (a). Formation of pyrrole-protein adducts (b) and cellular GSH content (c) in HSECs treated with retrorsine for 24 h in two-layer transwell co-culture model. Linear regression of HSEC viability with pyrrole-protein adduct level (d) or cellular GSH content (e) in HSECs after 24 h treatment of retrosine at different dosages (30, 60, and 120 μM). All individual values with retrorsine treatment are listed in Supplementary Table S2. The correlation was tested using Pearson's correlation analysis. Data are expressed as mean ± SD (n = 3). $*P < 0.05$, $**P < 0.01$.

3.2. PAs rely on the two-layer transwell co-culture model to exert their toxicity in HSECs

To evaluate the suitability of using the developed two-layer transwell co-culture model for the investigation of cytotoxic effects of PAs on HSECs, three PAs (retrorsine, monocrotaline and clivorine) representing both toxic types were tested. As the results shown in Fig. 3a, in the absence of HepaRG hepatocytes, even at significantly high concentration (1200 μM) for 24 h treatment, all three PAs did not affect viability of HSECs, indicating no cytotoxicity. In contrast, after 24 h treatment in the two-layer transwell co-culture model with co-culture of HSECs and HepaRG hepatocytes, significant decrease in HSEC viability in a concentration-dependent manner was observed for all three PAs. The results demonstrated that metabolic activation was essential for PAs to exert their cytotoxicity, and in the developed co-culture model, HepaRG hepatocytes were used to metabolically activate PAs to form dehydro-PAs, which diffused freely across the microporous membrane to act on HSECs leading to cytotoxicity in HSECs. Furthermore, the results demonstrated remarkably different toxic potency among three PAs with the lowest concentration of 300 μM for monocrotaline and 60 μM for both retrorsine and clivorine to significantly affect HSEC viability (Fig. 3a). The results demonstrated the successful development of a two-layer transwell co-culture model for the investigation of cytotoxicity and determination of toxic potency of different PAs in their target cell HSEC.

To investigate the reproducibility of the results obtained from the developed two-layer transwell co-culture model, four independent experiments were conducted to evaluate cytotoxicity of different concentrations of retrorsine in co-cultured HSECs at different concentrations and determine relative standard deviation (RSD) of cell viability. The results indicated a good reproducibility of the results with RSD ranging from 3.18 to 4.86 (Supplementary Table S1). In addition, using retrorsine as a representative PA, the formation of pyrrole-protein adducts and the change in cellular GSH content in HSECs, the comment phenomenons of PA-induced cytotoxicity (Yang et al., 2016) were also measured in this model. A concentration-dependent increase in pyrrole-protein adducts level and decrease in GSH content in HSECs were observed (Fig. 3b and c). These results were consistent with the previous findings in cells and animal studies (Ruan et al., 2015; Yang et al., 2016, 2017a, b). Moreover, Pearson's correlation analysis showed that there were strong correlations between the decreased cell viability and cellular pyrrole-protein adducts level, and between the decreased cell viability and cellular GSH content (Fig. 3d and e), suggesting for the first time that both formation of pyrrole-protein adducts and depletion of cellular GSH content might play important roles in PA-induced cytotoxicity in HSECs. Our findings with all the obtained results, including cell viability, formation of pyrrole-protein adducts, and cellular GSH content in HSECs treated with different concentrations of

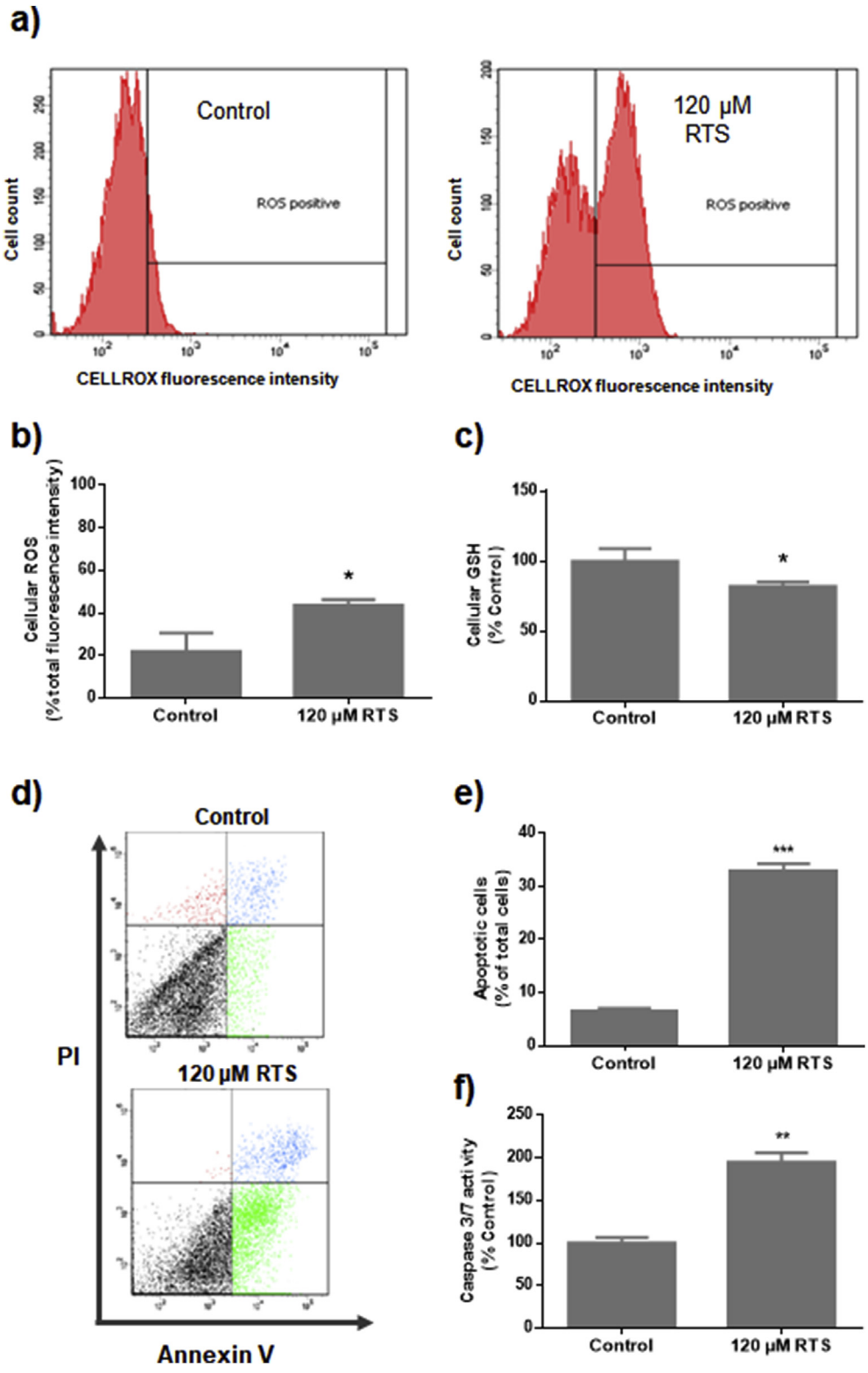

Fig. 4. Retrorsine-induced increase of cellular ROS and decrease of GSH content in HSECs after 3 h retrorsine (120 μM) treatment in two-layer transwell co-culture model: comparing with the control RTS-treated cells displayed an elevated fluorescence intensity, indicating increased ROS positive cells (a). Quantitative results of cellular ROS (b). The results of retrorsine-induced apoptosis in HSECs after 24 h retrorsine (120 μM) treatment in two-layer transwell co-culture model: flow cytometry analysis by double staining with FITC-labeled Annexin V/PI (d), quantitative results of apoptosis (e), and the results of caspase 3/7 activity (f). Data are expressed as mean ± SD (n = 3). $*P < 0.05$, $**P < 0.01$, $***P < 0.001$.

retrorsine for 24 h (Supplementary Table S2) further confirmed the successful development of the two-layer transwell co-culture model for study of PA-induced HSEC damage.

3.3. Retrorsine induces oxidative stress in HSECs

Previous studies have indicated a potential involvement of oxidative stress injury in the PA-induced hepatotoxicity (DeLeve et al., 1996; Ji et al., 2009; Zhao et al., 2011). We therefore examined reactive oxygen species (ROS) level, a marker of oxidative stress, in HSECs using the established two-layer transwell co-culture model. As shown in Fig. 4a and b, 4 h of retrorsine treatment caused a significant increase of ROS in HSECs, as evidenced by the elevation of CELLROX fluorescence intensity. The results also revealed the significant decrease in total GSH in HSECs (Fig. 4c), indicating that the impaired cellular anti-oxidative capabilities might contribute to the retrorsine-induced oxidative stress.

These direct findings of significantly increased ROS level and decreased GSH content in HSECs suggested that the involvement of oxidative stress would account for an important aspect in PA-induced hepatic sinusoidal damage.

3.4. Retrorsine induces apoptosis in HSECs

The type of cell death caused by retrorsine was further investigated by using the established two-layer transwell co-culture model. As shown in Fig. 4d and e, a feature of early apoptosis was observed by Annexin V/PI staining after 24 h treatment of retrorsine. Moreover, the increased caspase 3/7 activity further conformed retrorsine-induced apoptosis in HSECs (Fig. 4f). Taken together, all findings unambiguously demonstrated that apoptosis was responsible for retrorsine-induced cell death in HSECs.

4. Discussion

To date, researches on PA-induced HSEC damage have relied mainly on the animal models of PA-induced HSOS (Chen, 2009; DeLeve, 2013; DeLeve et al., 1999, 2003a). The difficulty in isolating HSECs of high purity, especially from these model animals that already developed hepatic sinusoidal damage, has limited the toxicity and mechanistic studies of PA-induced HSEC damage (DeLeve, 2013). The *in vitro* cell culture model has many advantages over animal models for investigative toxicology, but so far only limited *in vitro* studies have been conducted on HSECs. One of the main obstacles that impede the *in vitro* study on PA-induced HSEC damage is largely attributed to the extremely low or lack of expression of CYPs in human HSECs, in which PAs cannot be effectively bioactivated to dehydro-PAs leading to cytotoxicity (DeLeve, 2013). In fact, our results also showed that all three toxic PAs did not directly cause cytotoxicity in HSECs even at an excessively high concentration of 1200 μM, suggesting that PAs indeed require CYPs-mediated metabolic activation to exert their toxicity and HSECs with a lack of CYPs activity are not susceptible to the parent PAs (Fig. 3a). The other obstacle is that dehydro-PAs derived from different PAs are all highly unstable and are hardly synthesized, therefore, the direct *in vitro* test of different dehydro-PAs is extremely difficult (Cooper and Huxtable, 1996).

In order to solve these problems, in this study a novel two-layer transwell co-culture model was developed to evaluate the cytotoxicity of PAs on human HSECs. In our developed model, HepaRG hepatocytes and HSECs were isolated by the microporous membrane, which closely resembles hepatic microenvironment, where layers of hepatocytes and HSECs are separated by the space of Disse and blood diffuses freely in between (Poisson et al., 2017), and thus the results obtained would closely resemble the *in vivo* events. Three toxic PAs, including two retronecine-type and one otonecine-type PAs, were firstly used to validate the established two-layer co-culture transwell model for the investigation of PA-induced HSEC damage. The results unambiguously demonstrated that PAs could be metabolically activated by the co-cultured HepaRG hepatocytes to generate dehydro-PAs, which then move to and induce toxicity in the co-cultured HSECs. Moreover, the observed concentration-dependent cytotoxicity of three PAs with their different toxic potencies in HSECs further demonstrated the successful development of this *in vitro* model for the investigation of PA intoxication in HSECs. As shown in Fig. 3a, clivorine displayed the strongest cytotoxicity in co-cultured HSECs followed by retrorsine, while monocrotaline was the least toxic PA among these three PAs. This result was consistent with previous cytotoxic studies using HepaRG or HepaG2 cells to investigate relative cytotoxic potency of different PAs (Li et al., 2013; Allemang et al., 2018), further validating our developed *in vitro* model. It is noted that the toxic potencies of different PAs obtained via *in vitro* models are not always the same as those tested *in vivo* due to much more complicated *in vivo* situations including differences of PAs in absorption, distribution, metabolism in liver and other organs, and excretion processes. Nevertheless, the developed two-layer transwell co-culture model is an ideal platform for rapid evaluation of toxic potency of different PAs in HSECs and delineation of the detailed toxic mechanisms underlying PA-induced HSEC damage.

Subsequently, the developed two-layer co-culture transwell model was further used to study cytotoxic mechanism of a representative toxic PA retrorsine. The results revealed that dehydro-PA was generated from metabolic activation of retrorsine by the co-cultured HepaRG hepatocytes, then triggered GSH depletion, increased intracellular ROS, and formed pyrrole-protein adducts in HSECs, which eventually led to the apoptosis HSECs. Intracellular GSH is an important molecular which not only maintains cellular redox homeostasis by scavenging cellular ROS but also neutralizes (detoxifies) dehydro-PAs generated by metabolic activation of PAs (DeLeve et al., 1996; Ma et al., 2018). Therefore, GSH has been believed to play an important role in drug metabolism-induced liver injury (Deleve and Kaplowitz, 1991). Previous studies have demonstrated that PAs could cause significant GSH depletion in cells and animals and the toxicities caused by PAs could be rescued by restoration of cellular GSH (DeLeve et al., 1996; Yang et al., 2016). In the present study, the results illustrated that the decreased HSEC viability was in a good correlation with the decreased GSH level and elevated formation of pyrrole-protein adducts. Since GSH conjugation has been considered as a detoxification pathway by covalent binding dehydro-PAs to form readily excreted pyrrole-GSH conjugates, the diminished cellular GSH content impaired this detoxification pathway and exacerbated the formation of pyrrole-protein adducts, contributing to PA-induced HSEC damage. Moreover, our findings also revealed the increased cellular ROS level accompanied with a remarkable decrease of GSH content in HSECs after retrorsine treatment. This result was well correlated with the anti-oxidant role of GSH, because its depletion has been considered as a major cause for induction of cellular ROS. The formation of pyrrole-protein adducts, together with the decreased cellular GSH content and aggravated oxidative stress, eventually caused apoptosis of HSECs. All the results were consistent with previous studies in that PAs were demonstrated to significantly decrease cellular GSH in murine SECs (DeLeve et al., 1996), HepaG2 (Yang et al., 2016) and human liver L-02 cells (Ji et al., 2009), and produce dose-dependent formation of toxicity-related pyrrole-protein adducts in liver of mice and rats (Ruan et al., 2015; Yang et al., 2017b). It has been reported that apoptosis is one of the major mechanisms underlining PA-induced hepatotoxicity (Copple et al., 2004; Lu et al., 2018), while, our findings for the first time directly demonstrate that PAs could also induce apoptosis in HSECs. The detailed mechanism underlying PA-induced HSEC damage, however, remains to be further explored.

In conclusion, in the present study we mimicked the hepatic microenvironment and successfully developed and verified a novel two-layer transwell co-culture model that utilized two types of hepatic cells (HepaRG hepatocyte and HSECs) to study PA-induced HSEC damage. Like the *in vivo* scenario, based on the co-culture system, PAs indeed were bioactivated by HepaRG hepatocytes forming dehydro-PAs which subsequently damaged the adjacent HSECs. GSH depletion, pyrrole-protein adduction, and ROS elevation were proved to contribute to the PA-induced apoptosis in HSECs. This *in vitro* model enables us to investigate PA-induced HSEC injury in a more controllable *in vitro* condition and offers a new tool for a rapid screening and in-depth study of the detailed mechanisms of PA intoxication in HSECs. In addition, the developed model can also be used for *in vitro* screening other potential toxins that require hepatic metabolic activation prior to their intoxication on non-parenchymal liver cells, like HSECs.

Conflict of interest

All authors declare that they do not have anything to disclose regarding funding or conflict of interest with respect to this manuscript.

Declaration of interests

The authors declare that they have no known competing financial interests or personal relationships that could have appeared to influence the work reported in this paper.

Acknowledgements

The present study was supported by Research Grant Council of Hong Kong (GRF Grant no. 14110714) and CUHK Direct Grant (4054215). We sincerely thank Drs. Christiane Guguen-Guillouzo and Philippe Gripon from U522 INSERM and Dr. Christian Trepo from U271 INSERM for providing HepaRG cells.

Appendix A. Supplementary data

Supplementary data to this article can be found online at https://doi.org/10.1016/j.fct.2019.04.057.

Transparency document

Transparency document related to this article can be found online at https://doi.org/10.1016/j.fct.2019.04.057

References

Allemang, A., Mahony, C., Lester, C., Pfuhler, S., 2018. Relative potency of fifteen pyrrolizidine alkaloids to induce DNA damage as measured by micronucleus induction in HepaRG human liver cells. Food Chem. Toxicol. 121, 72–81.
Chen, M.Y., 2009. Reliable experimental model of hepatic veno-occlusive disease caused by monocrotaline (Retraction of vol 7 pg 395 2008). Hepatob. Pancreat. Dis. 8 396-396.
Cooper, R.A., Huxtable, R.J., 1996. A simple procedure for determining the aqueous half-lives of pyrrolic metabolites of pyrrolizidine alkaloids. Toxicon 34, 604–607.
Copple, B.L., Rondelli, C.M., Maddox, J.F., Hoglen, N.C., Ganey, P.E., Roth, R.A., 2004. Modes of cell death in rat liver after monocrotaline exposure. Toxicol. Sci. 77, 172–182.
Dehn, P.F., White, C.M., Conners, D.E., Shipkey, G., Cumbo, T.A., 2004. Characterization of the human hepatocellular carcinoma (HEPG2) cell line as an in vitro model for cadmium toxicity studies. In: Vitro Cell Dev-An, vol 40. pp. 172–182.
DeLeve, L.D., 2013. In: Liver Sinusoidal Endothelial Cells and Liver Injury. Drug-Induced Liver Disease, third ed. pp. 135–146.
DeLeve, L.D., Ito, Y., Bethea, N.W., McCuskey, M.K., Wang, X., McCuskey, R.S., 2003a. Embolization by sinusoidal lining cells obstructs the microcirculation in rat sinusoidal obstruction syndrome. Am. J. Physiol. Gastrointest. Liver Physiol. 284, G1045–G1052.
DeLeve, L.D., Wang, X., Tsai, J., Kanel, G., Strasberg, S., Tokes, Z.A., 2003b. Sinusoidal obstruction syndrome (veno-occlusive disease) in the rat is prevented by matrix metalloproteinase inhibition. Gastroenterology 125, 882–890.
Deleve, L.D., Kaplowitz, N., 1991. Glutathione metabolism and its role in hepatotoxicity. Pharmacol. Ther. 52, 287–305.
DeLeve, L.D., McCuskey, R.S., Wang, X., Hu, L., McCuskey, M.K., Epstein, R.B., Kanel, G.C., 1999. Characterization of a reproducible rat model of hepatic veno-occlusive disease. Hepatology 29, 1779–1791.
DeLeve, L.D., Shulman, H.M., McDonald, G.B., 2002. Toxic injury to hepatic sinusoids: sinusoidal obstruction syndrome (veno-occlusive disease). Semin. Liver Dis. 22, 27–41.
DeLeve, L.D., Wang, X.D., Kuhlenkamp, J.F., Kaplowitz, N., 1996. Toxicity of azathioprine and monocrotaline in murine sinusoidal endothelial cells and hepatocytes: the role of glutathione and relevance to hepatic venoocclusive disease. Hepatology 23, 589–599.
Edgar, J.A., Molyneux, R.J., Colegate, S.M., 2015. Pyrrolizidine alkaloids: potential role in the etiology of cancers, pulmonary hypertension, congenital anomalies, and liver disease. Chem. Res. Toxicol. 28, 4–20.
Fu, P.P., 2017. Pyrrolizidine alkaloids: metabolic activation pathways leading to liver tumor initiation. Chem. Res. Toxicol. 30, 81–93.
Fu, P.P., Chou, M.W., Xia, Q., Yang, Y., Yan, J., Doerge, D.R., Chan, P.C., 2001. Genotoxic pyrrolizidine alkaloids and pyrrolizidine alkaloid N-oxides - mechanisms leading to DNA adduct formation and tumorigenicity. J. Environ. Sci. Health, Part C: Environ. Carcinog. Ecotoxicol. 19, 353–385.
Fu, P.P., Xia, Q., Lin, G., Chou, M.W., 2004. Pyrrolizidine alkaloids–genotoxicity, metabolism enzymes, metabolic activation, and mechanisms. Drug Metab. Rev. 36, 1–55.
Gao, H., Ruan, J., Chen, J., Li, N., Ke, C., Ye, Y., Lin, G., Wang, J., 2015. Blood pyrrole-protein adducts as a diagnostic and prognostic index in pyrrolizidine alkaloid-hepatic sinusoidal obstruction syndrome. Drug Des. Dev. Ther. 9, 4861–4868.
Ji, L., Liu, T., Chen, Y., Wang, Z., 2009. Protective mechanisms of N-acetyl-cysteine against pyrrolizidine alkaloid clivorine-induced hepatotoxicity. J. Cell. Biochem. 108, 424–432.
Kang, Y.B., Rawat, S., Cirillo, J., Bouchard, M., Noh, H.M., 2013. Layered long-term co-culture of hepatocytes and endothelial cells on a transwell membrane: toward engineering the liver sinusoid. Biofabrication 5, 045008.
Kim, H.Y., Stermitz, F.R., Coulombe, R.A., 1995. Pyrrolizidine alkaloid-induced DNA-protein cross-links. Carcinogenesis 16, 2691–2697.
Lübberstedt, M., Müller-Vieira, U., Mayer, M., Biemel, K.M., Knöspel, F., Knobeloch, D., Nüssler, A.K., Gerlach, J.C., Zeilinger, K., 2011. HepaRG human hepatic cell line utility as a surrogate for primary human hepatocytes in drug metabolism assessment in vitro. J. Pharmacol. Toxicol. Methods 63, 59–68.
Li, N., Xia, Q., Ruan, J., Fu, P.P., Lin, G., 2011. Hepatotoxicity and tumorigenicity induced by metabolic activation of pyrrolizidine alkaloids in herbs. Curr. Drug Metabol. 12, 823–834.
Li, Y.H., Kan, W.L., Li, N., Lin, G., 2013. Assessment of pyrrolizidine alkaloid-induced toxicity in an in vitro screening model. J. Ethnopharmacol. 150, 560–567.
Lin, G., Cui, Y.Y., Hawes, E.M., 2000. Characterization of rat liver microsomal metabolites of clivorine, an hepatotoxic otonecine-type pyrrolizidine alkaloid. Drug Metab. Dispos. 28, 1475–1483.
Lin, G., Wang, J., Li, N., Li, M., Gao, H., Ji, Y., Zhang, F., Wang, H., Zhou, Y., Ye, Y., Xu, H., Zheng, J., 2011. Hepatic sinusoidal obstruction syndrome associated with consumption of Gynura segetum. J. Hepatol. 54, 666–673.
Lu, Y., Ma, J., Song, Z., Ye, Y., Fu, P.P., Lin, G., 2018. The role of formation of pyrrole-ATP synthase subunit beta adduct in pyrrolizidine alkaloid-induced hepatotoxicity. Arch. Toxicol. 92, 3403–3414.
Ma, J., Xia, Q., Fu, P.P., Lin, G., 2018. Pyrrole-protein adducts - a biomarker of pyrrolizidine alkaloid-induced hepatotoxicity. J. Food Drug Anal. 26, 965–972.
Mattocks, A.R., 1968. Toxicity of pyrrolizidine alkaloids. Nature 217, 723–728.
McGill, M.R., Yan, H.M., Ramachandran, A., Murray, G.J., Rollins, D.E., Jaeschke, H., 2011. HepaRG cells: a human model to study mechanisms of acetaminophen hepatotoxicity. Hepatology 53, 974–982.
Mohabbat, O., Srivastava, R.N., Younos, M.S., Merzad, A.A., Sediq, G.G., Aram, G.N., 1976. Outbreak of hepatic veno-occlusive disease in northwestern Afghanistan. Lancet 2, 269–271.
Poisson, J., Lemoinne, S., Boulanger, C., Durand, F., Moreau, R., Valla, D., Rautou, P.E., 2017. Liver sinusoidal endothelial cells: physiology and role in liver diseases. J. Hepatol. 66, 212–227.
Prakash, A.S., Pereira, T.N., Reilly, P.E.B., Seawright, A.A., 1999. Pyrrolizidine alkaloids in human diet. Mutat. Res. Genet. Toxicol. Environ. Mutagen 443, 53–67.
Robinson, O., Want, E., Coen, M., Kennedy, R., van den Bosch, C., Gebrehawaria, Y., Kudo, H., Sadiq, F., Goldin, R.D., Hauser, M.L., Fenwick, A., Toledano, M.B., Thursz, M.R., 2014. Hirmi Valley liver disease: a disease associated with exposure to pyrrolizidine alkaloids and DDT. J. Hepatol. 60, 96–102.
Roeder, E., 1995. Medicinal plants in Europe containing pyrrolizidine alkaloids. Pharmazie 50, 83–98.
Roeder, E., 2000. Medicinal plants in China containing pyrrolizidine alkaloids. Pharmazie 55, 711–726.
Ruan, J., Gao, H., Li, N., Xue, J., Chen, J., Ke, C., Ye, Y., Fu, P.P., Zheng, J., Wang, J., Lin, G., 2015. Blood pyrrole-protein adducts-A biomarker of pyrrolizidine alkaloid-induced liver injury in humans. J. Environ. Sci. Health, Part C: Environ. Carcinog. Ecotoxicol. 33, 404–421.
Ruan, J., Liao, C., Ye, Y., Lin, G., 2014a. Lack of metabolic activation and predominant formation of an excreted metabolite of nontoxic platynecine-type pyrrolizidine alkaloids. Chem. Res. Toxicol. 27, 7–16.
Ruan, J., Yang, M., Fu, P.P., Ye, Y., Lin, G., 2014b. Metabolic activation of pyrrolizidine alkaloids: insights into the structural and enzymatic basis. Chem. Res. Toxicol. 27, 1030–1039.
Smith, P.K., Krohn, R.I., Hermanson, G.T., Mallia, A.K., Gartner, F.H., Provenzano, M.D., Fujimoto, E.K., Goeke, N.M., Olson, B.J., Klenk, D.C., 1985. Measurement of protein using bicinchoninic acid. Anal. Biochem. 150, 76–85.
Wang, X.D., Kanel, G.C., DeLeve, L.D., 2000. Support of sinusoidal endothelial cell glutathione prevents hepatic veno-occlusive disease in the rat. Hepatology 31, 428–434.
Willmot, F.C., Robertson, G.W., 1920. Senecio disease, or cirrhosis of the liver due to senecio poisoning. Lancet 2, 848–849.
Xia, Q., Zhao, Y., Von Tungeln, L.S., Doerge, D.R., Lin, G., Cai, L., Fu, P.P., 2013. Pyrrolizidine alkaloid-derived DNA adducts as a common biological biomarker of pyrrolizidine alkaloid-induced tumorigenicity. Chem. Res. Toxicol. 26, 1384–1396.
Yan, C.C., Huxtable, R.J., 1995. Relationship between glutathione concentration and metabolism of the pyrrolizidine alkaloid, monocrotaline, in the isolated, perfused liver. Toxicol. Appl. Pharmacol. 130, 132–139.
Yang, M., Ruan, J., Fu, P.P., Lin, G., 2016. Cytotoxicity of pyrrolizidine alkaloid in human hepatic parenchymal and sinusoidal endothelial cells: firm evidence for the reactive metabolites mediated pyrrolizidine alkaloid-induced hepatotoxicity. Chem. Biol. Interact. 243, 119–126.
Yang, M., Ruan, J., Gao, H., Li, N., Ma, J., Xue, J., Ye, Y., Fu, P.P., Wang, J., Lin, G., 2017a. First evidence of pyrrolizidine alkaloid N-oxide-induced hepatic sinusoidal obstruction syndrome in humans. Arch. Toxicol. 91, 3913–3925.
Yang, X., Li, W., Sun, Y., Guo, X., Huang, W., Peng, Y., Zheng, J., 2017b. Comparative study of hepatotoxicity of pyrrolizidine alkaloids retrorsine and monocrotaline. Chem. Res. Toxicol. 30, 532–539.
Zhao, Y., Xia, Q., Yin, J.J., Lin, G., Fu, P.P., 2011. Photoirradiation of dehydropyrrolizidine alkaloids—formation of reactive oxygen species and induction of lipid peroxidation. Toxicol. Lett. 205, 302–309.
Zhao, Y., Xia, Q., da Costa, G.G., Yu, H., Cai, L., Fu, P.P., 2012. Full structure assignments of pyrrolizidine alkaloid DNA adducts and mechanism of tumor initiation. Chem. Res. Toxicol. 25, 1985–1996.
Zhu, L., Xue, J., Xia, Q., Fu, P.P., Lin, G., 2017. The long persistence of pyrrolizidine alkaloid-derived DNA adducts in vivo: kinetic study following single and multiple exposures in male ICR mice. Arch. Toxicol. 91, 949–965.